Acta Mech 228, 2741–2750 (2017)
DOI 10.1007/s00707-015-1517-x

ORIGINAL PAPER

Kuang-Chong Wu · Pei-Hsu Hsiao

A new boundary integral formulation for bending of anisotropic plates

Received: 1 March 2015 / Revised: 1 May 2015 / Published online: 14 December 2015

Abstract A new boundary integral formulation for the numerical solution of bending problems of anisotropic plates is proposed in this work. The formulation is based on a Stroh-like formalism for the classical plate theory. In contrast to the conventional formulation, which utilizes Betti's reciprocal work theorem with appropriate Green's functions, the proposed formulation makes use of Cauchy's integral theorem. An advantage of the new formulation is that it provides dual sets of boundary integral equations. With the dual sets, the integral equations to be solved can always be cast into the form of well-posed Fredholm integral equations of the second type for general boundary conditions. Another advantage is that all moment components on the boundary can be obtained without additional numerical differentiations. Numerical examples are given to demonstrate the effectiveness and efficiency of the proposed boundary integral formulation.

1 Introduction

The boundary element method enjoys a distinct advantage over domain type methods, such as the finite element method, as only the boundary needs to be discretized. Its application to solid mechanics problems started when Rizzo [1] presented an integral equation approach to boundary value problems of two-dimensional linear isotropic elasticity. An extension to anisotropic elasticity was made by Rizzo and Shippy [2]. If plane stress condition is considered, the two-dimensional problems are essentially related to the stretching of plates. The primary unknowns are the in-plane displacements and tractions.

The development of the boundary integral equation method for plate bending problems started relatively late as compared to that for plate stretching problems. A direct approach was employed by Bezine [3] and Stern [4] to obtain a general formulation of isotropic plate bending problems in terms of a pair of singular integral equations involving out-of-plane displacement, normal slope, bending moment, and shear on the plate boundary. The counterpart for an anisotropic plate was derived by Shi and Bezine [5]. All of the aforementioned works adopted a conventional boundary element formulation, which is based on Betti's reciprocal work theorem in conjunction with the appropriate fundamental solutions. The form of the integral equations for bending is quite different from that for stretching not only in the kernels but also in the presence of additional terms for plates with sharp corners. Furthermore, post-processing is required to compute boundary moments [6].

A different boundary integral equation formulation for two-dimensional elasticity problems was proposed by Wu et al. [7] based on distributions of body forces and dislocations. The new formulation consists of dual sets of boundary integral equations involving the tangential gradient of the displacements and tractions on the boundary. With the dual sets, the integral equations to be solved can always be cast into the form of well-posed Fredholm integral equations of the second type regardless of the types of boundary conditions. Another

K.-C. Wu (✉) · P.-H. Hsiao
Institute of Applied Mechanics, National Taiwan University, Taipei 106, Taiwan
E-mail: wukc@spring.iam.ntu.edu.tw

advantage is that the tangential displacement gradients and tractions together with Hooke's law can be used to compute the tangential stresses directly at the boundary.

The Stroh formalism is widely recognized as an elegant and powerful method for two-dimensional anisotropic elastostatics. A distinctive feature of the Stroh formalism is that the general solution is provided in terms of the eigenvalues and eigenvectors of a standard eigenvalue problem. The general solution contains two arbitrary complex functions for the plane stress or plate stretching problem. The functions can often be found by taking advantage of the orthogonality relations between the eigenvectors in conjunction with theories of analytic functions. Cheng and Reddy [8] established a Stroh-type formalism for the Kirchhoff anisotropic plates. A Stroh-like formalism for Kirchhoff bending theory of anisotropic plates was derived by Hwu [9] independently.

In [10], it was shown that the integral equations obtained by Wu et al. [7] are a direct consequence of analyticity of complex functions in Stroh's formalism for anisotropic elasticity. The objective of this work is, therefore, to set up boundary integral equations similar to those developed by Wu et al. [7] for the analysis of bending deformations in an anisotropic plate using the Stroh-like formalism proposed by Cheng and Reddy [8] and Hwu [9].

In the following discussions, a comma followed by a subscript α denotes the partial derivative with respect to x_α. A repeated index implies summation over the range from 1 to 2 unless otherwise specified.

2 Classical plate theory

Consider a thin plate of uniform thickness with the mid-plane located at $x_3 = 0$ in a Cartesian coordinate system. The classical plate theory assumes the following form for the displacement component U_i:

$$\begin{aligned} U_\alpha &= x_3\theta_\alpha(x_1, x_2), \\ U_3 &= w(x_1, x_2) \end{aligned} \tag{1}$$

where θ_α is the rotation and w is the deflection. The theory further suppresses the out-of-plane shear deformations so that

$$\theta_\alpha = -w_{,\alpha}. \tag{2}$$

The corresponding equilibrium equations are

$$\begin{aligned} M_{\alpha\beta,\beta} &= Q_\alpha, \\ Q_{\alpha,\alpha} + q &= 0 \end{aligned} \tag{3}$$

where q is the distributed lateral load per unit area in the x_3 direction on the plate surface, Q_α is the shear force, and $M_{\alpha\beta}$ is the moment. The plate is assumed to be made of a linear elastic material with possible variation of elastic constants in the thickness direction. The variation is further assumed to be symmetric about the middle surface of the plate so that there is no coupling between bending and extension. A laminate of multiple generally orthotropic layers that are symmetrically disposed about the middle surface is one example. The constitutive law of the plate is described by

$$M_{\alpha\beta} = D_{\alpha\beta\gamma\delta}\theta_{\gamma,\delta} \tag{4}$$

where $D_{\alpha\beta\gamma\delta}$ is the bending stiffness. From Eqs. (2), (3) and (4), the equation for the deflection w is

$$D_{\alpha\beta\gamma\delta}w_{,\alpha\beta\gamma\delta} = q. \tag{5}$$

3 Stroh-like formalism

In the absence of lateral load, $p = 0$, from Eq. (3), Q_α and $M_{\alpha\beta}$ can be expressed in terms of the stress function ψ_α as

$$Q_1 = -\eta_{,2}, \quad Q_2 = \eta_{,1}, \quad \eta = \psi_{\beta,\beta}/2, \tag{6}$$

$$M_{\alpha 1} = -\psi_{\alpha,2} - \lambda_{\alpha 1}\psi_{\beta,\beta}/2, \quad M_{\alpha 2} = \psi_{\alpha,1} - \lambda_{\alpha 2}\psi_{\beta,\beta}/2 \tag{7}$$

where $\lambda_{\alpha\beta}$ is defined as

$$\lambda_{11} = \lambda_{22} = 0, \quad \lambda_{12} = -\lambda_{21} = 1. \tag{8}$$

A set of first-order partial differential equations for $\boldsymbol{\theta}$ and $\boldsymbol{\psi}$ may be obtained by substituting Eqs. (6) and (7) into Eq. (4) as [9]

$$\begin{bmatrix} \boldsymbol{\theta}_{,2} \\ \boldsymbol{\psi}_{,2} \end{bmatrix} = \mathbf{N} \begin{bmatrix} \boldsymbol{\theta}_{,1} \\ \boldsymbol{\psi}_{,1} \end{bmatrix} \tag{9}$$

where

$$\mathbf{N} = \begin{bmatrix} \mathbf{N}_1 & \mathbf{N}_2 \\ \mathbf{N}_3 & \mathbf{N}_1^T \end{bmatrix}, \tag{10}$$

$$\mathbf{N}_1 = \begin{bmatrix} 0 & 1 \\ -\frac{D_{12}}{D_{22}} & -\frac{2D_{26}}{D_{22}} \end{bmatrix}, \quad \mathbf{N}_2 = \begin{bmatrix} 0 & 0 \\ 0 & \frac{1}{D_{22}} \end{bmatrix},$$
$$\mathbf{N}_3 = -\begin{bmatrix} D_{11} - \frac{D_{12}^2}{D_{22}} & 2\left(D_{16} - \frac{D_{12}D_{26}}{D_{22}}\right) \\ 2\left(D_{16} - \frac{D_{12}D_{26}}{D_{22}}\right) & 4\left(D_{66} - \frac{D_{26}^2}{D_{22}}\right) \end{bmatrix}. \tag{11}$$

The general solution of $\boldsymbol{\theta}$ and $\boldsymbol{\psi}$ is given by

$$\begin{bmatrix} \boldsymbol{\theta} \\ \boldsymbol{\psi} \end{bmatrix} = 2\mathrm{Re}\left(\sum_{\alpha=1}^{2} f_\alpha\left(z_\alpha\right) \boldsymbol{\xi}_\alpha^{(r)}\right) \tag{12}$$

where $z_\alpha = x_1 + p_a x_2$, p and $\boldsymbol{\xi}^{(r)}$ are, respectively, the eigenvalue and right eigenvector of $\mathbf{N}$. Conversely, the function $f_K(z_K)$ may be expressed in terms of $\boldsymbol{\theta}$ and $\boldsymbol{\psi}$ as

$$f_\alpha(z_\alpha) = \left(\boldsymbol{\xi}_\alpha^{(\ell)}\right)^T \begin{bmatrix} \boldsymbol{\theta} \\ \boldsymbol{\psi} \end{bmatrix} \tag{13}$$

where $\boldsymbol{\xi}_\alpha^{(\ell)}$ is the left eigenvector of $\mathbf{N}$. It may be shown that

$$\boldsymbol{\xi}^{(r)} = \begin{bmatrix} \mathbf{a} \\ \mathbf{b} \end{bmatrix}, \quad \boldsymbol{\xi}^{(\ell)} = \begin{bmatrix} \mathbf{b} \\ \mathbf{a} \end{bmatrix} \tag{14}$$

where $\mathbf{a}$ and $\mathbf{b}$ are 2×1 matrices.

4 Boundary integral equations

It is well known that a complex analytic function f, defined in a closed region R enclosed by a smooth contour Γ, can be expressed in terms of its values on Γ by Cauchy's integral formula as

$$\gamma f(z) = \frac{1}{2\pi i} \int_\Gamma \frac{f(\zeta)}{\zeta - z} \mathrm{d}\zeta \tag{15}$$

where $z = x_1 + ix_2$, $\zeta = \xi_1 + i\xi_2$, $i = \sqrt{-1}$, $\boldsymbol{\xi} = (\xi_1, \xi_2) \in \Gamma$, $\gamma = 1$ if $\mathbf{x} = (x_1, x_2) \in R$, $\gamma = 1/2$ if $\mathbf{x} \in \Gamma$ and the principal value of the integral must be taken. The direction of integration in Eq. (15) is counterclockwise. Since z_α may be expressed as $z_K = y_1 + iy_2$, where $y_1 = x_1 + \mathrm{Re}[p_\alpha]x_2$ and $y_2 = \mathrm{Im}\,[p_\alpha]\,x_2$. Eq. (15) may be generalized for $f_\alpha(z_\alpha)$ or its derivative $f'_\alpha(z_\alpha)$ as

$$\begin{aligned} \gamma f'_\alpha(z_\alpha) &= \frac{1}{2\pi i} \int_\Gamma \frac{f'_\alpha(\zeta_\alpha)}{\zeta_\alpha - z_\alpha} \mathrm{d}\zeta_\alpha \\ &= \frac{1}{2\pi i} \int_\Gamma \frac{1}{\zeta_\alpha - z_\alpha} \frac{\partial f_\alpha(\zeta_\alpha)}{\partial \sigma} \mathrm{d}\sigma(\boldsymbol{\xi}) \end{aligned} \tag{16}$$

where $\zeta_\alpha = \xi_1 + p_\alpha \xi_2$ and $d\sigma = \sqrt{d\xi_1^2 + d\xi_2^2}$.

Equation (12) with Eqs. (13) and (16) gives [10]

$$\gamma \frac{\partial}{\partial s}\begin{bmatrix}\boldsymbol{\theta}\\ \boldsymbol{\psi}\end{bmatrix} = \mathrm{Im}\left(\sum_{\alpha=1}^{2}\frac{\hat{z}_\alpha}{\pi}\int_\Gamma \frac{\boldsymbol{\xi}_\alpha^{(r)}\left(\boldsymbol{\xi}_\alpha^{(\ell)}\right)^T}{\zeta_\alpha - z_\alpha}\frac{\partial}{\partial \sigma}\begin{bmatrix}\boldsymbol{\theta}\\ \boldsymbol{\psi}\end{bmatrix} d\sigma(\boldsymbol{\xi})\right) \tag{17}$$

where s is the arc length along a certain contour C, and $\hat{z}_\alpha = dx_1/ds + p_\alpha dx_2/ds$. If the contour C is taken to coincide with the boundary contour Γ, Eq. (17) yields the following dual sets of boundary integral equations:

$$\frac{1}{2}\mathbf{d}(\mathbf{x}) = \int_\Gamma (-\mathbf{W}(\mathbf{x},\boldsymbol{\xi})\mathbf{d}(\boldsymbol{\xi}) + \mathbf{U}(\mathbf{x},\boldsymbol{\xi})\mathbf{t}(\boldsymbol{\xi}))\, d\sigma(\boldsymbol{\xi}), \tag{18}$$

$$\frac{1}{2}\mathbf{t}(\mathbf{x}) = \int_\Gamma \left(\mathbf{V}(\mathbf{x},\boldsymbol{\xi})\mathbf{d}(\boldsymbol{\xi}) - \mathbf{W}(\mathbf{x},\boldsymbol{\xi})^T\mathbf{t}(\boldsymbol{\xi})\right) d\sigma(\boldsymbol{\xi}) \tag{19}$$

where $\mathbf{d} = \partial\boldsymbol{\theta}/\partial s$, $\mathbf{t} = -\partial\boldsymbol{\psi}/\partial s$, and

$$\mathbf{W}(\mathbf{x},\boldsymbol{\xi}) = -\frac{1}{\pi}\mathrm{Im}\left[\sum_{\alpha=1}^{2}\frac{\hat{z}_\alpha}{\zeta_\alpha - z_\alpha}\mathbf{a}_\alpha\mathbf{b}_\alpha^T\right],$$

$$\mathbf{U}(\mathbf{x},\boldsymbol{\xi}) = -\frac{1}{\pi}\mathrm{Im}\left[\sum_{\alpha=1}^{2}\frac{\hat{z}_\alpha}{\zeta_\alpha - z_\alpha}\mathbf{a}_\alpha\mathbf{a}_\alpha^T\right],$$

$$\mathbf{V}(\mathbf{x},\boldsymbol{\xi}) = -\frac{1}{\pi}\mathrm{Im}\left[\sum_{\alpha=1}^{2}\frac{\hat{z}_\alpha}{\zeta_\alpha - z_\alpha}\mathbf{b}_\alpha\mathbf{b}_\alpha^T\right]. \tag{20}$$

It is remarkable that Eqs. (18) and (19) are in exactly the same forms as those for two-dimensional elasticity problems given in [7]. For two-dimensional elasticity problems, **d** and **t** are, respectively, the in-plane displacement gradient and traction along the boundary. For plate bending problems, however, **d** is related to the rotation gradients along the boundary, and **t**, from Eqs. (6) and (7), is given by

$$\mathbf{t} = M_{nn}\mathbf{n} + M_{ns}^*\mathbf{s}, \quad M_{ns}^* = M_{ns} - \eta \tag{21}$$

where **n** and **s**, respectively, are the outward unit normal vector and unit tangential vector on the boundary Γ,

$$M_{nn} = M_{\alpha\beta}n_\alpha n_\beta, \quad M_{ns} = M_{\alpha\beta}n_\alpha s_\beta, \tag{22}$$

and M_{ns}^* is connected to the effective shear force by

$$V_n = \frac{\partial M_{ns}^*}{\partial s}. \tag{23}$$

In contrast, the conventional boundary integral equations employ w, $\theta_n = \partial w/\partial n$, M_{nn} and V_n. It should also be noted that for plates with sharp corners, M_{ns} on the boundary may be piecewise continuous with possible jumps at the corners, but Eqs. (18) and (19) remain valid for boundary points other than the corner points. However, the concentrated corner forces associated with the jumps in M_{ns} appear explicitly as extra terms in the conventional boundary integral equations.

Equations (18) and (19) may be used to construct a set of well-posed Fredholm integral equations of the second type for general boundary conditions. Let the boundary conditions at a boundary point **x** be specified as

$$\mathbf{X}(\mathbf{x})\mathbf{t}(\mathbf{x}) - \mathbf{Y}(\mathbf{x})\mathbf{d}(\mathbf{x}) = \tilde{\mathbf{t}}(\mathbf{x}) \tag{24}$$

where $\tilde{\mathbf{t}}$ contains given boundary data, **X** and **Y** are 2×2 diagonal matrices whose elements are either one or zero and $\mathbf{X} + \mathbf{Y} = \mathbf{I}$, **I** being the unit matrix. Define

$$\tilde{\mathbf{d}}(\mathbf{x}) = \mathbf{X}(\mathbf{x})\mathbf{d}(\mathbf{x}) - \mathbf{Y}(\mathbf{x})\mathbf{t}(\mathbf{x}). \tag{25}$$

Equations (17) and (18) with Eqs. (24) and (25) yield

$$\frac{1}{2}\tilde{\mathbf{d}}(\mathbf{x}) = \int_{\Gamma} \left(-\tilde{\mathbf{W}}(\mathbf{x}, \boldsymbol{\xi})\tilde{\mathbf{d}}(\boldsymbol{\xi}) + \tilde{\mathbf{U}}(\mathbf{x}, \boldsymbol{\xi})\tilde{\mathbf{t}}(\boldsymbol{\xi}) \right) \mathrm{d}\sigma(\boldsymbol{\xi}) \tag{26}$$

where

$$\tilde{\mathbf{W}}(\mathbf{x}, \boldsymbol{\xi}) = -\frac{1}{\pi}\mathrm{Im}\left[\sum_{\alpha=1}^{2} \frac{\hat{z}_\alpha}{\zeta_\alpha - z_\alpha}\tilde{\mathbf{a}}_\alpha(\mathbf{x})\tilde{\mathbf{b}}_\alpha^T(\boldsymbol{\xi})\right],$$
$$\tilde{\mathbf{U}}(\mathbf{x}, \boldsymbol{\xi}) = -\frac{1}{\pi}\mathrm{Im}\left[\sum_{\alpha=1}^{2} \frac{\hat{z}_\alpha}{\zeta_\alpha - z_\alpha}\tilde{\mathbf{a}}_\alpha(\mathbf{x})\tilde{\mathbf{a}}_\alpha^T(\boldsymbol{\xi})\right], \tag{27}$$

and

$$\tilde{\mathbf{a}}_\alpha(\mathbf{x}) = \mathbf{X}(\mathbf{x})\mathbf{a}_\alpha + \mathbf{Y}(\mathbf{x})\mathbf{b}_\alpha, \quad \tilde{\mathbf{b}}_\alpha(\mathbf{x}) = \mathbf{Y}(\mathbf{x})\mathbf{a}_\alpha + \mathbf{X}(\mathbf{x})\mathbf{b}_\alpha. \tag{28}$$

$\tilde{\mathbf{a}}_\alpha(\boldsymbol{\xi})$ and $\tilde{\mathbf{b}}_\alpha(\boldsymbol{\xi})$ are also defined by Eq. (28) but with $\mathbf{X}$ and $\mathbf{Y}$ associated with the boundary conditions at the boundary point $\boldsymbol{\xi}$. Equation (26) is the desired equation for $\tilde{\mathbf{d}}$, which contains the "missing" boundary data. For traction boundary conditions ($\mathbf{X} = \mathbf{I},\ \mathbf{Y} = \mathbf{0}$), Eq. (26) is simply Eq. (17), and for displacement boundary conditions ($\mathbf{X} = \mathbf{0},\ \mathbf{Y} = \mathbf{I}$), Eq. (26) is the same as Eq. (18).

5 Numerical formulation

Equation (26) is a Cauchy-type singular integral equation. The singular integral equation may be solved numerically by discretizing the boundary into N line elements where it is assumed that $\mathbf{d}^* = \tilde{\mathbf{d}}_k^*$ and $\mathbf{t}^* = \tilde{\mathbf{t}}_k^*$ on the kth element, $k = 1 \sim N$, where $\tilde{\mathbf{d}}_k^*$ and $\tilde{\mathbf{t}}_k^*$ are the constant values of $\mathbf{d}^*$and $\mathbf{t}^*$evaluated at the center of the kth element. The system of algebraic equations resulting from Eq. (26) for $\tilde{\mathbf{d}}_k^*$ is

$$\sum_{k=1}^{N} \mathbf{G}_{jk}\tilde{\mathbf{d}}_k^* = \sum_{k=1}^{N} \mathbf{H}_{jk}\tilde{\mathbf{t}}_k^*, \quad j = 1 \sim N \tag{29}$$

where for $j \neq k$,

$$\mathbf{G}_{jk} = \frac{1}{\pi}\mathrm{Im}\left[\sum_{\alpha=1}^{2} \frac{\hat{z}_\alpha^{(j)}}{\hat{z}_\alpha^{(k)}} \log\left(\frac{z_\alpha^{(k+1)} - z_\alpha^{(j+1/2)}}{z_\alpha^{(k)} - z_\alpha^{(j+1/2)}}\right)\tilde{\mathbf{a}}_\alpha^{(j)}\left(\tilde{\mathbf{b}}_\alpha^{(k)}\right)^T\right],$$
$$\mathbf{H}_{jk} = -\frac{1}{\pi}\mathrm{Im}\left[\sum_{\alpha=1}^{2} \frac{\hat{z}_\alpha^{(j)}}{\hat{z}_\alpha^{(k)}} \log\left(\frac{z_\alpha^{(k+1)} - z_\alpha^{(j+1/2)}}{z_\alpha^{(k)} - z_\alpha^{(j+1/2)}}\right)\tilde{\mathbf{a}}_\alpha^{(j)}\left(\tilde{\mathbf{a}}_\alpha^{(k)}\right)^T\right], \tag{30}$$

$\mathbf{G}_{kk} = \mathbf{I}/2$ and $\mathbf{H}_{kk} = \mathbf{0}$. In Eq. (30),

$$\hat{z}_\alpha^{(j)} = \cos\theta^{(j)} + p_\alpha \sin\theta^{(j)}, \quad \theta^{(j)} = \tan^{-1}\left(\frac{x_2^{(j+1)} - x_2^{(j)}}{x_1^{(j+1)} - x_1^{(j)}}\right),$$
$$z_\alpha^{(k)} = x_1^{(k)} + p_\alpha x_2^{(k)}, \quad z_\alpha^{(j+1/2)} = \frac{1}{2}\left(z_\alpha^{(j+1)} + z_\alpha^{(j)}\right),$$
$$\tilde{\mathbf{a}}_\alpha^{(j)} = \mathbf{X}\left(\mathbf{x}^{(j)}\right)\mathbf{a}_\alpha + \mathbf{Y}\left(\mathbf{x}^{(j)}\right)\mathbf{b}_\alpha, \quad \tilde{\mathbf{b}}_\alpha^{(j)} = \mathbf{Y}\left(\mathbf{x}^{(j)}\right)\mathbf{a}_\alpha + \mathbf{X}\left(\mathbf{x}^{(j)}\right)\mathbf{b}_\alpha \tag{31}$$

where $\left(x_1^{(k)}, x_2^{(k)}\right)$ and $\left(x_1^{(k+1)}, x_2^{(k+1)}\right)$ are the end points of the kth element. Note that in the treatment outlined above the singular integrals are analytically integrated, and hence no numerical integrations of singular integrals are needed.

Once $\mathbf{d}$ and $\mathbf{t}$ are all determined, any moment or curvature components in the interior of the plate can be computed using Eq. (17) with $\gamma = 1$. Moreover, any moment or curvature components on the boundary may be obtained with $\mathbf{d}$ and $\mathbf{t}$ in conjunction with the normal derivatives of $\boldsymbol{\theta}$ and $\boldsymbol{\psi}$ on the boundary computed by

$$\frac{\partial}{\partial n}\begin{bmatrix}\boldsymbol{\theta}\\ \boldsymbol{\psi}\end{bmatrix} = \mathrm{Re}\left[\sum_{\alpha=1}^{2}\frac{n_1+n_2p_\alpha}{-n_2+n_1p_\alpha}\boldsymbol{\xi}_\alpha^{(r)}\left(\boldsymbol{\xi}_\alpha^{(\ell)}\right)^T\right]\begin{bmatrix}\mathbf{d}\\ -\mathbf{t}\end{bmatrix} \tag{32}$$

where

$$\frac{\partial\boldsymbol{\psi}}{\partial n} = (M_{ns}+\eta)\,\mathbf{n} + M_s\mathbf{s}. \tag{33}$$

For example, the twisting moment M_{ns} is calculated as

$$M_{ns} = \frac{1}{2}\left(\mathbf{n}^T\frac{\partial\boldsymbol{\psi}}{\partial n} + \mathbf{s}^T\mathbf{t}\right). \tag{34}$$

Equation (26) is for plates subjected to edge loads and hence cannot be directly applied to laterally loaded plates. For plates loaded laterally by $q(x_1, x_2)$, however, one may express the deflection w as [11]

$$w = w_0 + w^* \tag{35}$$

where w_0 is a particular solution satisfying Eq. (5). With Eq. (35), one only needs to solve for w^*, which is free from the lateral load. The decomposition of deflection described by Eq. (35) works well for distributed loads. For more general loading such as concentrated forces, Eq. (26) must be extended to account for the loading explicitly. The extension is in progress and will be reported in a separate communication.

6 Examples

To illustrate the effectiveness of the proposed formulation, Equation (26) was applied numerically to solve the problem of a square plate of side length $2a$, as shown in Fig. 1, which is simply supported on all edges and is subjected to a uniform load q. The particular solution w_0 in Eq. (35) was taken as

$$w_0 = \frac{q}{24D_{11}}\left(x_1^4 - 6a^2x_1^2 + 5a^4\right), \tag{36}$$

which represents the deflection of a uniformly loaded strip parallel to the x_1 axis. It satisfies Eq. (5) and the boundary conditions at $x_1 = \pm a$. The boundary conditions for w^* as described by Eq. (24) are

$$\begin{aligned}&\tilde{\mathbf{t}}^* = \mp\frac{q}{2D_{11}}\left(x_1^2 - a^2\right)\begin{bmatrix}1\\ D_{12}\end{bmatrix}, \quad \mathbf{X} = \begin{bmatrix}0 & 0\\ 0 & 1\end{bmatrix}, \quad \text{at } x_2 = \pm a,\\ &\tilde{\mathbf{t}}^* = \mathbf{0}, \quad \mathbf{X} = \begin{bmatrix}1 & 0\\ 0 & 0\end{bmatrix}, \quad \text{at } x_1 = \pm a.\end{aligned} \tag{37}$$

Equation (29) was constructed and solved by dividing the boundary of the plate equally into $N = 80$ line elements with the corners included as end points.

The materials considered were an isotropic material with $E = 1\,\mathrm{GPa}$ and $v = 0.3$ and an orthotropic material with $E_1 = 181\,\mathrm{GPa}$, $E_2 = 10.3\,\mathrm{GPa}$, $G = 7.17\,\mathrm{GPa}$, $\nu_1 = 0.28$. Equation (29) cannot be applied directly to isotropic materials for which the eigenvalue $p = i$ is repeated. Instead, the isotropic material was regarded as a slightly orthotropic material with $E_1 = 1\,\mathrm{GPa}$ and $E_2 = 0.999\,\mathrm{GPa}$ so that the corresponding eigenvalues become $p = 0.9846i, 1.0162i$. The eigenvalues of the orthotropic material are $p = \pm 1.1238 + 1.7114i$. The variations of $\kappa_{11} = -w_{,11}$, which is the curvature of the deflected middle surface in the x_1 direction, and the bending moment M_{22} at $x_2 = 0$ were calculated using Eq. (17) with $\gamma = 1$. The variations of $\kappa_{22} = -w_{,22}$, which is the curvature of the deflected middle surface in the x_2 direction, and the bending moment M_{11} at $x_2 = 0$ were calculated using Eq. (32). The results computed by the boundary integral equations (bie) are shown in Figs. 2 and 3 for the isotropic material and Figs. 4 and 5 for the orthotropic material. Because of symmetry, the results are presented for $x_1 > 0$ only. For comparison, the corresponding exact solutions for

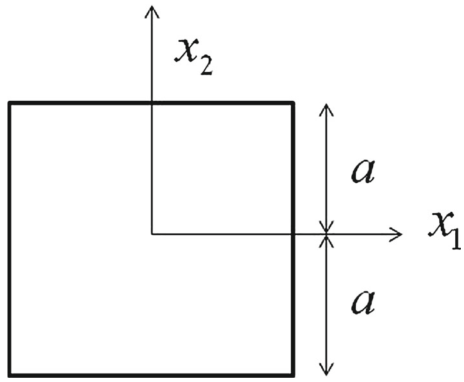

Fig. 1 A square plate of side length $2a$

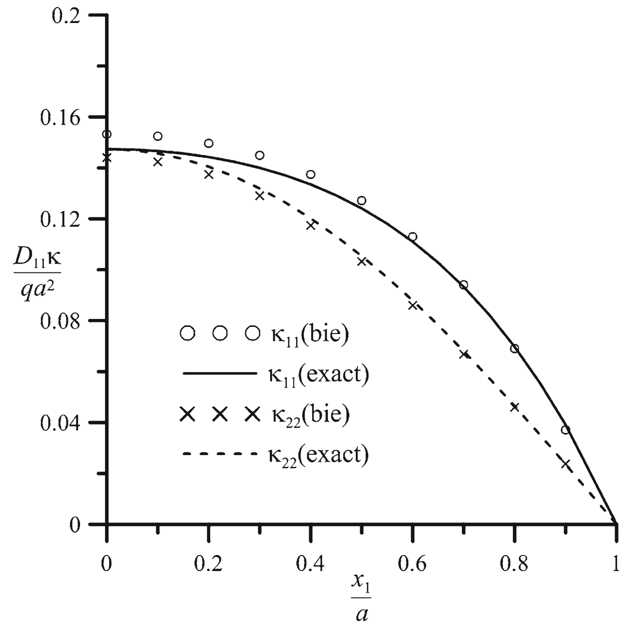

Fig. 2 Curvatures at $x_2 = 0$ for the isotropic material

the isotropic material and the orthotropic material are also given. The exact solutions for the isotropic material were obtained from the following series solution of the deflection [11]:

$$w = \frac{64qa^2}{\pi^5 D_{11}} \sum_{m=1,3,5\ldots}^{\infty} \frac{1}{m^5} \left[\left(1 - \frac{\alpha_m \tanh \alpha_m + 2}{2\cosh \alpha_m} \cosh \frac{\alpha_m x_2}{a} \right) + \frac{1}{2\cosh \alpha_m} \frac{\alpha_m x_2}{a} \cosh \frac{\alpha_m x_2}{a} \right] \sin \alpha_m \left(1 + \frac{x_1}{a} \right) \tag{38}$$

where $\alpha_m = m\pi/2$. Those for the orthotropic material were derived from [12],

$$w = \frac{64qa^2}{\pi^5 D_{11}} \sum_{m=1,3,5\ldots}^{\infty} \frac{1}{m^5} \mathrm{Re} \left[1 + \frac{s_2^2}{s_1^2 - s_2^2} \frac{1}{\cosh \alpha_m s_1} \cosh \left(\alpha_m s_1 \frac{x_2}{a} \right) - - \frac{s_1^2}{s_1^2 - s_2^2} \frac{1}{\cosh \alpha_m s_2} \cosh \left(\alpha_m s_2 \frac{x_2}{a} \right) \right] \sin \alpha_m \left(1 + \frac{x_1}{a} \right), \tag{39}$$

where $s_\alpha = -ip_\alpha$.

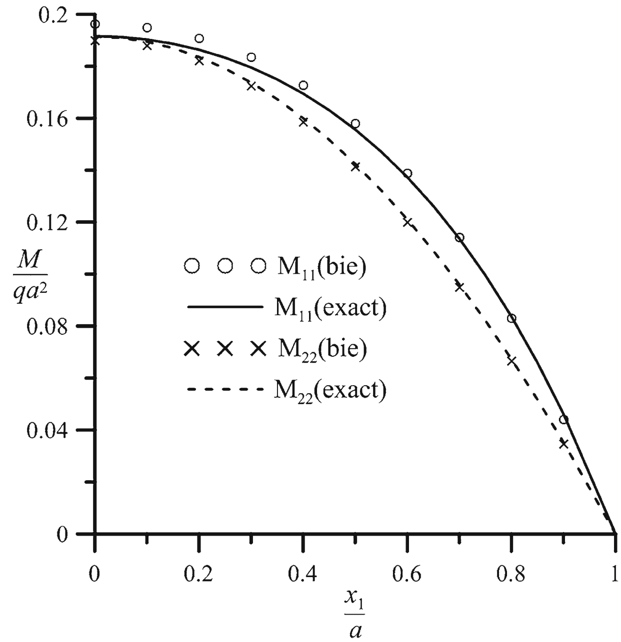

Fig. 3 Moments at $x_2 = 0$ for the isotropic material

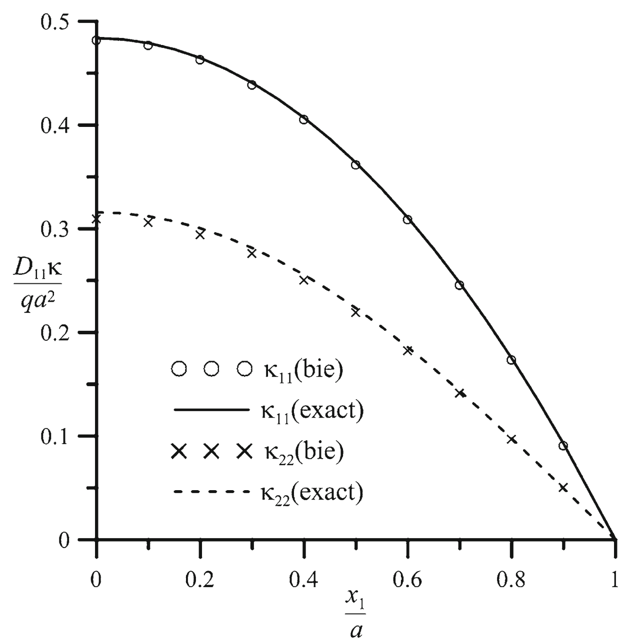

Fig. 4 Curvatures at $x_2 = 0$ for the orthotropic material

In general, the numerical results shown in Figs. 2, 3, 4, 5 are in close agreement with the analytic results. In particular, computed values of curvatures and moments at the center, $x_1 = 0$ and $x_2 = 0$, of the plate and the relative errors are shown in Table 1. For the isotropic material, the numerical results of κ_{11} and M_{11} appear larger than the analytic ones, but those of κ_{22} and M_{22} are smaller. For the orthotropic material, either curvatures or bending moments are smaller than the exact solutions. The largest error of 3.88 % occurs in the case of κ_{11} for the isotropic material. However, the error of κ_{11} for the orthotropic material is −0.40 % and is the smallest. The approaches of the numerical results to the exact solutions do not seem to follow any definite trends.

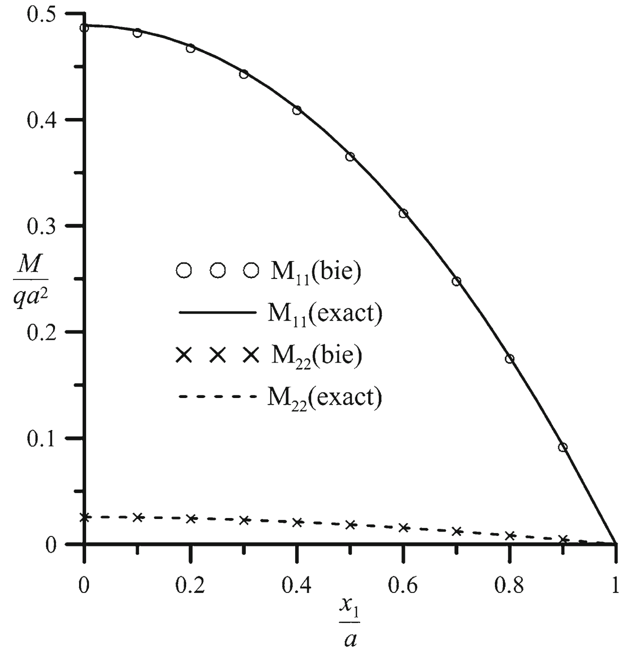

Fig. 5 Moments at $x_2 = 0$ for the orthotropic material

Table 1 Computed values at the center $x_1 = 0$, $x_2 = 0$ and the relative errors

	Isotropic	Orthotropic
$D_{11}\kappa_{11}/qa^2$	0.1530 (3.88 %)	0.4818 (−0.40 %)
$D_{11}\kappa_{22}/qa^2$	0.1440 (−2.28 %)	0.3094 (−2.02 %)
M_{11}/qa^2	0.1963 (2.46 %)	0.4868 (−0.42 %)
M_{22}/qa^2	0.1447 (−0.84 %)	0.0253 (−1.53 %)

7 Conclusions

A new boundary integral formulation for anisotropic plate bending problems has been developed. The new formulation yields dual sets of boundary integral equations so that the integral equations to be solved can always be cast into the form of well-posed Fredholm integral equations of the second type for general boundary conditions. The boundary integral equations are in exactly the same forms as those for two-dimensional elasticity problems, but contain rotation gradients and moments as unknowns. The equations are applicable to plates with or without sharp corners. Moreover, all moment components on the boundary can be obtained without additional numerical differentiations.

References

1. Rizzo, F.J.: An integral equation approach to boundary value problems of classical elastostatics. Q. Appl. Math. **25**, 83–95 (1967)
2. Rizzo, F.J., Shippy, D.J.: A method for stress determination in plane anisotropic elastic bodies. J. Compos. Mater. **4**, 36–61 (1970)
3. Bezine, G.: Boundary integral formulation for plate flexure with arbitrary boundary conditions. Mech. Res. Commun. **5**, 197–206 (1978)
4. Stern, M.: A general boundary integral formulation for the numerical solution of plate bending problems. Int. J. Solids Struct. **15**, 769–782 (1979)
5. Shi, G., Bezine, G.: A general boundary integral formulation for the anisotropic plate bending problems. J. Compos. Mater. **22**, 694–716 (1988)
6. dos Reis, A., Albuquerque, É.L., Torsani, F.L., Palermo, L., Sollero, P.: Computation of moments and stresses in laminated composite plates by the boundary element method. Eng. Anal. Bound. Elem. **35**, 105–113 (2011)
7. Wu, K.C., Chiu, Y.T., Hwu, Z.H.: A new boundary integral equation formulation for linear elastic solids. ASME J. Appl. Mech. **59**, 344–348 (1992)

8. Cheng, Z.Q., Reddy, J.N.: Octet formalism for Kirchhoff anisotropic plates. Proc. R. Soc. Lond. A **458**, 1499–1517 (2002)
9. Hwu, C.: Stroh-like formalism for the coupled stretching–bending analysis of composite laminates. Int. J. Solids Struct. **40**, 3681–3705 (2003)
10. Wu, K.C., Chen, C.T.: Stress analysis of anisotropic elastic v-notched bodies. Int. J. Solids Struct. **33**, 2403–2416 (1996)
11. Timoshenko, S., Woinowsky-Krieger, S.: Theory of Plates and Shells. McGraw-Hill, New York (1959)
12. Lekhnitskii, S.G.: Anisotropic Plate. Gordon and Breach, London (1968)